

Mg II Absorbing Galaxies: Halos or Disks?

JANE C. CHARLTON¹

Astronomy and Astrophysics Department
Pennsylvania State University, University Park, PA 16802
email: *charlton@astro.psu.edu*

CHRISTOPHER W. CHURCHILL

Board of Studies in Astronomy and Astrophysics
University of California, Santa Cruz, Santa Cruz, CA 95064
email: *cwc@ucolick.org*

Accepted for publication: *Astrophysical Journal*

ABSTRACT

We challenge the conventional view that the majority of Mg II/Lyman limit absorbers are extended halos of galaxies comprised of “clouds” with near-unity covering factor. The gaseous disks of spiral galaxies are known to extend to large radii and likely contribute a significant cross-section for absorption. We perform a Monte-Carlo survey of QSO fields in which the model galaxies have Mg II absorbing “clouds” in a spherical halo or in a randomly oriented disk. For both geometries, models that recover the observed properties of Mg II absorbers have only a 70–80% covering factor. Therefore, regardless of absorber geometry, a survey of randomly selected QSO fields should yield a non-negligible number of non-absorbing galaxies at small impact parameters. Very few have been observed (Steidel 1995). However, selection effects are important, and once the observational procedures are applied to our model fields we find that this result is expected. Since both spherical halo and disk models can be made consistent with survey results, we present tests for discerning the geometric distribution of absorbing gas from *Hubble Space Telescope* images and high resolution spectra.

Subject headings: quasars: absorption lines — galaxies: structure — galaxies: evolution

¹Center for Gravitational Physics and Geometry, Pennsylvania State University

1. Introduction

Quasar absorption lines (QALs) provide unique, sensitive, and direct probes of the gaseous content in galaxies over look-back times comparable to a Hubble time. Studies of QALs promise to contribute insights into the processes that regulate the evolution of galaxies and the mechanisms that determine the physical conditions in interstellar and halo clouds. The gas in galaxies is a key ingredient to their on-going evolution, yet virtually nothing is known about the gaseous conditions in early-epoch galaxies, and how these conditions evolve to the present time. The field of QSO absorption lines has matured quite rapidly in the last half-decade. As such, a reasonably sized database, from which we can draw inferences about the general properties of galaxies known to give rise to absorption, has accumulated.

Low resolution spectroscopic surveys of the resonant CIV $\lambda\lambda 1548, 1550$ and MgII $\lambda\lambda 2976, 2803$ doublets (Sargent, Boksenberg, & Steidel 1988, Sargent, Steidel, & Boksenberg 1988, Steidel & Sargent 1992) have established the statistical nature and evolution of various “populations” of absorbers. The evolution of the population selected by the presence of MgII is virtually indistinguishable from the population selected by the presence of a Lyman limit break. This comes as little surprise, since MgII is known to trace HI gas that is optically thick at the Lyman limit (Bergeron & Stasińska 1986, Steidel & Sargent 1992). Follow-up imaging surveys of MgII absorbers have been highly successful at detecting a galaxy at the redshift seen in absorption (Bergeron & Boissé 1991, Steidel 1995). The associated galaxies are seldom fainter than $0.1 L_K^*$ and span the full range of galaxy types (Steidel, Dickinson, & Persson 1994, Steidel 1995, Drinkwater, Webster, & Thomas 1995). However, galaxies in the same cluster as the QSO provide an exception to the rule that *every* bright galaxy produces MgII absorption (Bechtold & Ellingson 1992). This could occur more generally in galaxy clusters where ram pressure or high energy ionization fields act to destroy extended low ionization gaseous components.

It has become apparent that these various populations are likely the absorption signatures of various regions and conditions within galaxies. Indeed, the survey data have been used to infer the statistical properties of a “typical” MgII absorbing galaxy at intermediate redshifts (Steidel 1993a). Such a galaxy

is characterized by an inner region of radius ~ 15 kpc that gives rise to damped Ly α lines, a region extending to ~ 40 kpc that produces MgII absorption and a Lyman limit break, and an outer region extending to ~ 70 kpc that is less shielded from the extragalactic background radiation and produces absorption lines in higher ions such as CIV. Beyond these inferences drawn from statistical cross-section arguments, there has been little direct information on which parts of galaxies give rise to MgII absorption. Studies through the Galactic Halo (Savage 1993, Savage, Lu, & Sembach 1995, Sembach, Savage, & Lu 1995) have provided results which suggest that complex dynamical disk/halo interactions may give rise to MgII absorbing gas. These processes may have analogs in external galaxies, but definitive interpretations of absorption from the Galaxy are lacking due to our difficult vantage point. Bowen, Blades, & Pettini (1995a,b) examined UV spectra and images (often in several bands, including X-ray and HI) of local MgII absorbing galaxies. They often found that it is a challenge to unambiguously identify the substructures giving rise to MgII absorption in these nearby systems, which often showed some sign of past interaction or were accompanied by satellite galaxies. In other words, the environments around the galaxies were not always isolated enough to clearly determine with which object the gas was actually associated. In the case of a line of sight through M81 and the Galaxy, each of which have satellite galaxies affecting their environments, the MgII absorption profile is blended with a 400 km s^{-1} spread. A further important lesson from their study is the possibility of altogether mis-identifying the absorbing galaxy. In the case of Q1543 + 489, two galaxies with velocity separation 120 km s^{-1} are absorber candidates. The first has impact parameter $45h^{-1}$ kpc, and the second $83h^{-1}$ kpc. This latter galaxy is outside the range probed by existing intermediate redshift imaging surveys, and as such, would be completely missed. Indeed, such surveys would likely claim they had successfully identified the former galaxy as the absorber. Such mis-identifications or ambiguities, even if they are relatively infrequent, may have an impact on inferences drawn from small number statistics, such as the fraction of non-absorbing galaxies at small impact parameters.

Ultimately, the kinematic-rich high resolution absorption spectra obtainable with 10-meter class telescopes and the high spatial resolution Hubble Space

Telescope (HST) images should aid the quest to understand (in individual cases) which types and parts of galaxies give rise to MgII absorption. Indeed, high resolution spectra have provided some leverage for examining statistical correlations between host galaxy properties and absorbing gas kinematics (also chemical and ionization conditions). Lanzetta and Bowen (1992) studied five absorbing galaxies at resolutions of 7 and 35 km s⁻¹ and found some profiles to be consistent with the signatures expected from a simple rotating structure and some that match predictions from infall/outflow within a spherically symmetric structure. Additionally, they found preliminary evidence that the profile complexity and the strength of absorption are correlated with impact parameter (eg. only one or two subcomponents at larger impacts). However, as concluded by Bowen, Blades, & Pettini (1995b) from their study of nearby galaxies (where high spatial resolution data are available and evidence for interactions has been seen), generalized models of halos may be misleading. Detailed models of many individual systems may provide a database from which a more general understanding of absorbing gas can be obtained. Churchill, Vogt, & Steidel (1995) presented a preliminary study of a striking HIRES (Vogt 1994) profile from Q1331 + 170, and suggest that quasi-symmetric outflowing structures (eg. superbubbles) may be present in what appears to be two close galaxies. Unfortunately, such a model can never be demonstrated to be a unique interpretation of the data. Clearly, even with HST images to corroborate inferences based upon high resolution spectral data, a large sample will need to be compiled before a comprehensive understanding of the spatial distribution, motions, and origins of galactic substructures giving rise to MgII absorption is developed.

Nonetheless, now that a database of MgII absorbing galaxy properties (eg. luminosities, optical/IR colors, redshifts, and impact parameters) is becoming available (Steidel, Dickinson, & Persson 1996, hereafter SDP), we can begin to learn something about the absorbing gas and its relation to the host galaxy. Though the high resolution spectra provide detailed information about the absorbing gas, existing low resolution absorption line data are proving to be sufficient for developing a basic appreciation of the conditions under which the presence of MgII is expected.

1.1. This Paper

In this paper, we are motivated by the basic question: “what is the general *geometric* cross-section of MgII absorbing gas in and around galaxies?” What we really aim to learn is if a single geometric cross-section can be invoked to help predict the presence or non-presence of absorption once a galaxy’s general properties and line of sight impact to the QSO are known. The conventional wisdom is that MgII absorption is produced in effectively spherical extended halos [dating from Bahcall & Spitzer (1969)]. Recent support for this view has been presented by Steidel (1995) (hereafter S95), who has demonstrated that the physical extent of MgII absorbing gas around galaxies scales with rest *K* luminosity following a Holmberg-like relationship (Holmberg 1975)

$$R(L_K) = 38h^{-1} (L_K/L_K^*)^{0.15} \text{ kpc} \quad (1)$$

(cf. Fig. 2 in S95). The S95 paper presents preliminary results from the extensive study of SDP which is still in progress. One striking result to date is that of 58 absorbing galaxies and 14 non-absorbing galaxies measured, there are only two non-absorbing galaxies “below the $R(L_K)$ line” given by this relationship (i.e. only two galaxies have line of sight impact parameters that fall within the now predicted surrounding absorbing region and do not exhibit absorption). Also, in only three cases is the identified absorbing galaxy found “above the $R(L_K)$ line”. The most straight-forward interpretation is that MgII absorbing gas is distributed with a roughly spherical cross-section, and has a nearly unity covering factor down to the Steidel & Sargent (1992) survey equivalent width limit $W_0(\lambda 2796) \sim 0.3 \text{ \AA}$ with a *K* luminosity (mass) dependent “cut-off boundary”. This conclusion is supported in part by the notion that a disk-like geometry, of random orientation, presents a significantly smaller statistical cross-section such that a non-negligible number of non-absorbers below the $R(L_K)$ line would have been detected.

However, these simple geometric models deserve further consideration, since there is clear evidence for “clumpiness” in the absorbing gas. Though Lanzetta & Bowen (1990) found that $W_0(\lambda 2796)$ and the impact parameter *D* of the absorbing galaxies follow the “smooth” relation $W_0 \propto D^{-\alpha}$ with $\alpha = 0.92 \pm 0.16$, S95 has shown that in fact there is a large scatter, which is not consistent with the tight correlation expected to arise from a smooth distribution of

halo gas (cf. Fig. 3 of S95). Since intermediate and high resolution absorption lines typically exhibit multiple absorption subcomponents (Petitjean & Bergeron 1990, Lanzetta & Bowen 1992), we infer that a near-unity covering factor must result from absorbing gas distributed in discrete clumps which each have a minimum equivalent width W_{\min} set by the physics of photoionized diffuse gas. We also note that the evidence for unity covering factor is statistical – in any single case it is not possible to be certain that the galaxy identified at the same redshift as that seen in MgII absorption is indeed the galaxy responsible for the absorption.

We will demonstrate that galaxy disks with realistic aspect ratios contribute a geometric cross-section for MgII absorption competitive with that of spherical halos. We also examine the possibility that observed absorption properties may actually be governed to a large extent by gas distributed in a disk geometry. In §3 we describe Monte-Carlo simulations of populations of galaxies with absorbing gas distributed in spherical and in disk geometries, and compare these models to the observed impact parameters, luminosities, and equivalent widths in the SDP survey. A careful consideration of the selection procedures, given in §4, is essential to the interpretation of our model results. In §5, we present simple predictions, to help distinguish whether absorption often arises primarily in the disks themselves, based upon forthcoming high spatial resolution HST images of the absorbing galaxies and from high resolution spectra of the absorption lines. The basic results of our Monte-Carlo study of the cross-section of MgII absorption are summarized in the concluding §6.

2. The Statistical Contribution of Disk Geometries

It is expected that some fraction of the MgII absorbing galaxies likely result from lines of sight through the disks of Milky Way-like galaxies. High velocity clouds in the Halo have a covering factor of at most 38% [through half the halo (Savage, Lu, & Sembach 1995, Bowen, Blades, & Pettini 1995a)], and thus by themselves do not provide a near-unity covering factor. Further, Bowen, Blades, & Pettini (1995a) find that a significant fraction of the high velocity clouds are kinematically consistent with disk co-rotation, so that they all may not really be a halo component *per se*, but instead be more closely asso-

ciated with the disk.

Since roughly 80% of field galaxies² have disks, we consider the MgII absorption cross-section contributed by a randomly oriented population of disks. In fact, a disk embedded in a sphere of the same radius ($R_d/R_h = 1$) presents a significant cross-section. An infinitely thin disk yields a lower limit of $1/2$ for the relative probability for intersecting a disk relative to a sphere. When the disk thickness is increased, or the condition $R_d/R_h = 1$ is relaxed, this probability increases rapidly. We define the disk thickness $T = h/R_d$, where h is the half-thickness of the disk, and derive the relative probability for intersection of a population of randomly oriented disks with respect to spheres of radius R_h ,

$$P(T, R_d/R_h) = (T + 0.5) \left(\frac{R_d}{R_h} \right)^2. \quad (2)$$

As illustrated in Fig. 1, to achieve equal cross-section contributions from a population of disks and spheres, the absorbing gas in a disk need only extend $\sim 20\%$ beyond that in a spherical structure for reasonable thickness. Values of $T = 0.2 - 0.3$ are plausible for the outer, warped extensions of galaxy disks (Diplas & Savage 1991), since a disk with a scale-height of 5 kpc would likely have a significant amount of *absorbing* gas at twice that height. Furthermore, it is not unreasonable to conjecture that MgII absorbing gas in these regions could be as extended or even more extended than a distribution of MgII absorbing gas in a halo, given that the HI necessary for photoionization shielding is likely more concentrated in the plane defining the disk.

It is also important to consider what the effective covering factor, down to some equivalent width limit, would be for a population of disks. We suggest that the equivalent width is likely to increase with disk inclination because the increased pathlength through an inclined disk yields increased column densities and a larger velocity dispersion of absorbing clouds, since the number intercepted is proportional to pathlength. A simple increase in column density increases $W_0(\lambda 2796)$ most effectively when absorption falls on the linear part of the curve of growth. A curve of growth analysis reveals that, near the equivalent width limit of 0.3 \AA , absorption is on the linear part of the curve of growth for $b \geq 20 \text{ km s}^{-1}$. Doppler

²The presence of MgII absorption does select the population of field galaxies (Bergeron & Boissé 1991, Steidel 1993a).

parameters on this order are quite common in the intermediate resolution ($\sim 30 \text{ km s}^{-1}$) spectra of Petitjean & Bergeron (1990), and are consistent with the idea that low resolution data sample the velocity dispersion of a few or more individual clouds along the line of sight. For $W_0(\lambda 2796) \geq 0.6 \text{ \AA}$, it is even more likely that the number of clouds intercepted and their velocity dispersion dominates the value of the equivalent width. Petitjean & Bergeron (1990) find that $W_0(\lambda 2796)$ still scales linearly with the number of resolved subcomponents.

Ultimately, the extent of the disk contribution to the overall cross-section for MgII absorption depends upon the detailed physics of sharp HI edges (gas dynamical processes, ionization field and strength, galaxy mass and shape, external pressure) (Maloney 1993, Corbelli & Salpeter 1993, Dove & Shull 1994). Locally, extended HI disks (beyond the optical radius) are common [cf. the recent review by Irwin (1995) and references therein], but only in a few cases has the $N(\text{HI})$ distribution been mapped down to a sensitivity below the expected sharp edge at which the gas converts from mostly neutral to mostly ionized (Corbelli, Schneider, & Salpeter 1989, van Gorkom *et al.* 1993). In NGC 3198, the $N(\text{HI})$ distribution is observed to drop sharply with radius for $N(\text{HI}) < 5 \times 10^{19} \text{ cm}^{-2}$ (van Gorkom *et al.* 1993), but is still 10^{18} cm^{-2} at 35–40 kpc. This rapid decline is likely to slow at larger radii. Bowen, Blades, & Pettini (1995b) find that there exists a correlation between the B magnitude of spiral galaxies and their HI radii measured from 21-cm emission. Their application of the Holmberg-like relation $R(\text{HI}) = R^*(L_B/L_B^*)^\beta$ to local HI disks provides evidence that β becomes less steep as the $N(\text{HI})$ threshold is decreased, and approaches the values required to match the intermediate redshift MgII absorbers, namely $\beta \sim 0.2$ [for B luminosity (S95)] at the Lyman limit, $N(\text{HI}) \sim 10^{17.3} \text{ cm}^{-2}$. Although it may be an extreme example, we also note that in the M81 interacting group there is a large covering factor of material with $N(\text{HI}) > 10^{20} \text{ cm}^{-2}$ beyond a radius of 40 kpc around M81 itself, which is spread throughout the group in a flattened distribution (Yun, Ho, & Lo 1994).

In the Milky Way, $N(\text{HI}) > 10^{19} \text{ cm}^{-2}$ at a galactocentric radius of 30 kpc in the direction $l = 130^\circ$ (Diplas & Savage 1991). By extrapolating this value using their observed radial scale-length of 5.5 kpc in this direction, we obtain $N(\text{HI}) = 10^{17} \text{ cm}^{-2}$ at a

radius of ~ 60 kpc. HST spectra of various QSOs, Active Galactic Nuclei, and Halo stars, looking in various directions through the Galaxy, show MgII absorption arising in the disk (Savage 1993, Lu, Savage, & Sembach 1994, Cardelli, Sembach, & Savage 1995, Sembach, Savage, & Lu 1995), though the radial extent of the MgII itself is not observed directly. In some cases, the absorbing gas could actually be associated with an $N(\text{HI})$ even smaller than 10^{17} cm^{-2} [at high redshift MgII is found to be associated only with systems that are optically thick at the Lyman limit, but at low redshift the ionizing background is reduced and some MgII systems are observed with τ_{LL} somewhat less than unity (Bergeron *et al.* 1994)]. Thus, in the Milky Way, it might even be expected that the MgII disk extends well beyond 50 kpc. To make all this plausible, metals would have to exist at these large radii, either by the action of galactic fountains, by infall of debris from satellites, or because they were present in the material from which the galaxy was formed.

Based upon these arguments, we suggest that the cross-section contribution of thick and/or extended disks and their related material (eg. co-rotating clouds) may well be large enough to account for the majority of MgII absorbers. Realistically, absorbers are probably quite diverse, including contributions from LMC-like satellites, streaming tidal debris formed in merging events, occasional τ_{LL} low surface brightness galaxies, and even early-type galaxies of sufficient K luminosity [the latter two having been observed in the SDP survey (Steidel, private communication)].

3. Modeling Absorbing Galaxies

We perform Monte-Carlo simulations that allow us to predict the numbers and properties of absorbing and non-absorbing galaxies in a sample of randomly generated fields centered on QSOs. We have designed the simulations so that our results can be compared to observations. Since the SDP survey represents the most comprehensive observational program to date, we briefly describe their work [but also see Drinkwater, Webster, and Thomas (1995)].

Drawing primarily from the Sargent, Steidel, & Boksenberg (1988) and Steidel & Sargent (1992) surveys, SDP obtained optical and IR images of 51 QSO fields in which 58 MgII absorbers had been detected ($0.3 \leq z \leq 0.9$) and of 25 “control” fields in which the QSO spectra exhibit no absorption to a completeness

limit of $W_0(\lambda 2796) = 0.3 \text{ \AA}$. The images were taken over a large range of band passes and the detection levels were targeted to ~ 2 magnitudes fainter than present day L^* for the known absorption redshifts. A combination of filters were used in order that the rest-frame B magnitude of the galaxies could be measured. Additionally, K band images were obtained for all fields. Confirmation of any absorbing galaxies identified in the imaging portion of the program required follow-up spectroscopy. Unless a field had several identified candidates, spectra were obtained in a pattern from small angular separation to larger until a match was found for the redshift seen in absorption. This follow-up spectroscopy in most fields is nearly complete within a $8-10''$ radius of the QSO. For control fields, redshifts were obtained for nearly all galaxies in the images within $10''$ of the QSO. Preliminary results from this study are summarized in S95.

For our model fields, the redshifts, luminosities, and impact parameters are known for *all* galaxies within $10''$ of the field center. The fraction of absorbing and non-absorbing model galaxies is thus representative of an unbiased sample of QSO fields. Our procedure is as follows: The galaxy redshift is selected at random in the range $0.3 \leq z \leq 0.9$, roughly matching the observed distribution. The redshift determines the physical size of the region (corresponding to a radius of $10''$) within which this galaxy will be located³. The galaxy luminosity L_K is selected from a Schechter function,

$$P(L_K)dL_K \sim (L_K/L_K^*)^\alpha \exp[-(L_K/L_K^*)] dL_K, \quad (3)$$

with $\alpha = -1.0$. This is derived from the value, $\alpha = -0.7$, observed for the luminosity function of the absorption-selected sample (S95), which is then weighted inversely by the absorbing cross-section area of a galaxy to obtain the true luminosity function. The galaxy is located randomly within the $10''$ region surrounding the QSO, giving the impact parameter D . The ‘‘observed’’ equivalent width W_0 along the line of sight is then determined based on the assumed geometry and model parameters. If the generated W_0 exceeds the 0.3 \AA observation threshold, then the galaxy is designated as an ‘‘absorber’’, and otherwise as a ‘‘non-absorber’’.

³The conversion assumes $q_0 = 0$. All sizes quoted throughout this paper would be $\sim 80\%$ smaller for $q_0 = 0.5$.

3.1. Spherical Models

Invoking a spherical geometry, S95 suggested that the relatively sharp observed cut-off in the size of MgII absorbing regions may be provided by the decrease of the pressure of diffuse gas that confines the clouds responsible for MgII absorption within the halo. When the pressure decreases below a threshold value, which scales with the mass of the galaxy, the column density of HI in an individual cloud is no longer sufficient to shield MgII and keep it in its singly ionized state. This effect roughly sets a minimum column density for *individual clouds*, for as the pressure decreases outward from the galaxy center, $N(\text{HI})$ of the clouds decreases (Mo 1995). This column density limit apparently corresponds to an equivalent width of $0.15 - 0.30 \text{ \AA}$, since weaker absorbers are rarely observed (Steidel & Sargent 1992, Churchill 1996). To investigate this supposition, we ran a series of photoionization models, CLOUDY (Ferland 1988), and computed the equivalent widths of model clouds. These models were plane parallel slabs illuminated from one side with continuum slope $\alpha_{\text{ox}} = -1.5$. For the range of ionization parameters $-4.0 \leq \log \Gamma \leq -1.0$, the average equivalent width was 0.13 \AA for $\tau_{\text{LL}} \sim 1$ clouds with $\log N(\text{HI}) \sim 17.5 \text{ cm}^{-2}$.

Empirically, the distribution of equivalent widths is roughly consistent with a power law (Steidel & Sargent 1992),

$$n(W_0)dW_0 \sim W_0^{-\delta}dW_0, \quad (4)$$

where $\delta = 1.65 \pm 0.90$, and thus many absorption systems have total W_0 near this limiting equivalent width. The relationship between the sum of the column densities and the observed equivalent width depends upon the distribution of velocities of clouds along the line of sight. Intermediate resolution spectroscopy reveals that the equivalent width increases almost linearly with the number of components (Pettitjean & Bergeron 1990). Thus, it is reasonable to assume that for the low resolution spectra, the individual clouds are sufficiently dispersed in velocity space so that their equivalent widths add to a total observed equivalent width W_0 for the MgII absorber.

The challenge for designing realistic spherical cloud models is to produce a near-unity covering factor when a typical line of sight at large impact is likely to pass through only one or two clouds. If this is the case, then some lines of sight will certainly fail to pass through any clouds observable in MgII, resulting in non-absorbers.

3.1.1. Design and Parameters

Guided by this general picture, we design models of a distribution of clouds in a spherical halo, governed by the following parameters: (1) a mean number of clouds $N_c(0)$ along a line of sight through the halo with impact parameter $D = 0$, (2) a power law dependence of the equivalent width of an individual cloud on the radius from sphere center, $W(R) \sim R^{-\alpha}$, that would result from a decrease in the individual cloud column densities due to decreasing pressure with increasing R , (3) a variable cloud size factor, given as the variance σ of a Gaussian distribution centered on $W(R)$, and (4) a mean minimum limiting equivalent width W_{\min} for an individual cloud.

For a line of sight at impact parameter D , the number of clouds $N_c(D)$ is determined by scaling $N_c(0)$ by the pathlength through a sphere of radius $R(L_K)$ [given by Eq. (1)]. In each model we choose either $W_{\min} = 0.15 \text{ \AA}$ or 0.30 \AA . For the former, the mean number of clouds at $R(L_K)$ is set equal to two, and for the latter to one, so that the mean W_0 at $R(L_K)$ is 0.30 \AA in either case. The value of $R(L_K)$ is determined using $\beta = 0.15$ to match observations (S95), however, we adjust the normalization R^* to minimize the sum of the number of non-absorbers below and the number of absorbers above the $R(L_K)$ line given by Eq. (1). This iterative process results in self-consistent models. The actual number of clouds along the particular line of sight is selected from a Poisson distribution with mean $N_c(D)$. The locations of the clouds are chosen at random along the line of sight (no dependence of cloud density on R), and the power law index α is used to compute $W(R)$. The actual individual cloud equivalent width W_c is selected from a Gaussian distribution with variance σ centered on $W(R)$. The ‘‘observed’’ equivalent width W_0 is determined by summing the W_c , an approximation justified by the nearly one to one correlation seen between equivalent width and the number of subcomponents in an absorption line (Petitjean & Bergeron 1990). A successful model should recover the observed equivalent width distribution $n(W_0)dW_0$. In order to roughly constrain our models, we assume a power law distribution and determine the least squares fit slope δ to the distribution of model W_0 .

3.1.2. Absorption Properties

Table 1 lists the various series of model parameters and the fractions of absorbers above f_{above} and below

f_{below} the $R(L_K)$ boundary [shown in Fig. 2 and given by Eq. (1)] for an unbiased sample of fields. In fact, the fraction f_{below} gives the covering factor within radius $R(L_K)$. From models S1–S4, we see that δ is strongly dependent on the value of α , but that α has little effect on the covering factor. There is a strong dependence of δ on the mean number of clouds along a line of sight (models S5–S7). The dependence of these gross properties on σ is minimal (compare models S3 and S6). By increasing the number of clouds $N_c(0)$, the covering factor f_{below} can be increased such that it is quite close to unity, and α can be chosen so that the observed value of $\delta \sim 1.65$ is obtained. In these spherical cloud models, large W_0 result from multiple clouds along a line of sight and/or from a large value of α . Table 1 illustrates the balance between the parameters $N_c(0)$ and α . For $\alpha = 2$, we can obtain $\delta = 1.6$ (enough large W_0) with a mean of only two clouds at $D = 0$ (model S11). For $\alpha = 0.5$, a mean of three clouds is necessary (model S2).

The covering factor could be further increased by using an even larger $N_c(0)$, but then there would be too many large W_0 values (δ would be too small for any $\alpha > 0$). This problem is less severe if W_{\min} is reduced from 0.30 \AA to 0.15 \AA (compare models S7 and S10), but the lack of observed small W_{\min} values, discussed above, indicates that 0.15 \AA is really a limit on how far down this parameter can be pushed. For models S2, S11, and S12, we set $N_c(0) = 3, 2,$ and $6,$ and tuned W_{\min}, α and σ to match the observed $n(W_0)dW_0$ distribution. These three models will be used in the following sections to illustrate variations between different realizations of spherical cloud models.

The predicted distribution of impact parameter D versus K luminosity is illustrated in Figs. 2(a–c) for three different randomly selected realizations of model S2. To facilitate some level of comparison to Fig. 2 of S95, we plot 58 random absorbing galaxies. The number of non-absorbers (63) presented on this figure is the mean number that would arise in the same number of fields that yield a mean of 58 absorbers. At first glance, the lack of a clean demarcation of absorbers and non-absorbers around the $R(L_K)$ line appears inconsistent with the SDP data. As we will address in §4, the appearance and subsequent interpretation of a D versus L_K diagram may be quite sensitive to observational selection procedures. In fact, models S2 and S12 succeed fairly well in that they yield a large value of f_{below} and a small value of f_{above} . How-

ever, we note that this is not the case for all spherical cloud models that we can design. For example, Table 1 shows that in model S11 a much larger fraction (0.34) of the galaxies below the $R(L_K)$ line will be non-absorbers and a much larger fraction (0.22) of the galaxies above the $R(L_K)$ line will be absorbers. In these models, absorbing galaxies can exist above the $R(L_K)$ line because of the Poisson fluctuations in the number of clouds along the line of sight and the Gaussian spread around the equivalent width of a single cloud. From Table 1, we infer that the parameter $N_c(0)$ is the most critical in determining the value of f_{above} . For $N_c(0) = 2$ the value of $N_c(D)$ will decrease slowly with D and the probability of detecting one cloud can be significant for an impact greater than $D = R(L_K)$.

In Figs. 3(a–c), we also illustrate the distributions of W_0 versus D for the three realizations presented in Figs. 2(a–c). These diagrams illustrate that our approach to modeling “clumpiness” within the absorbers manifests in a $W_0 - D$ distribution qualitatively consistent with the data presented in Fig. 3 of S95. The scatter in the diagram at a given D value is produced by the variation of the number of clouds along a line of sight, and the various locations (in galactocentric distance R) at which clouds are intercepted.

3.2. Disk Models

Expected properties of absorbing gas in galaxy disks should be guided by impressions of the thick, warped outer disk regions of nearby spirals, as we have discussed in §2. There are likely to be clumps and irregularities (“clouds”) in the disk (Irwin 1995, and references therein). The number of clouds and their overall velocity dispersion is likely to increase with increased pathlength through an inclined disk. Based upon the conclusions of Bowen, Blades, & Pettini (1995b) that the extent of MgII absorbing gas in disks is likely follow the Holmberg-like relation for B luminosity with $\beta \sim 0.2$, we assume that absorbing gas in disks roughly follows Eq. (1) for K luminosity with $\beta = 0.15$.

3.2.1. Design and Parameters

The parameters for our disk models are: (1) a power law dependence of $W(R)$ on the radius in the disk, given by

$$W(R) = 0.3 (R/R_{0.3})^{-\alpha} \text{ \AA}, \quad (5)$$

where $R_{0.3}$ is the radius at which a line of sight perpendicular to the disk would yield $W_0 = 0.3 \text{ \AA}$ on average, (2) a “clumpiness” factor, given as the variance σ of a Gaussian distribution centered on $W(R)$, and (3) a “cut-off radius” R_{cut} beyond which $W(R)$ effectively vanishes, which could be somewhat larger than $R_{0.3}$ for the less severe ionization conditions likely at low redshifts (Bergeron *et al.* 1994).

In order to determine W_0 for a given line of sight, the disk is randomly oriented with inclination i [with probability $P(i)di \sim \sin(i)di$]. The line of sight is located at a random angle θ from the major axis of the ellipse representing the inclined disk projected onto the plane of the sky. The radial position where the line of sight pierces the plane of the disk is then

$$R = D \left[\cos^2 \theta + \left(\frac{\sin \theta}{\cos i} \right)^2 \right]^{1/2}. \quad (6)$$

The equivalent width $W(R)$ is given by Eq. (5) scaled by the increased pathlength factor $\sec(i)$ to roughly account for the combined effects of higher line of sight column density and velocity dispersion of the absorbing clouds. The “observed” W_0 is then selected from a Gaussian distribution with variance σ centered on $W(R)$. From physical principles, we expect a sharp cut-off at some radius in the MgII absorbing gas, so we assign a cut-off radius in the range $1.5 \leq R_{\text{cut}}/R_{0.3} \leq 2$ (except for one model with $R_{\text{cut}} = \infty$, chosen for purposes of illustration). As with the spherical models, we normalize Eq. (1) with $\beta = 0.15$ by minimizing the sum of the number of non-absorbers below and the number of absorbers above the $R(L_K)$ line.

3.2.2. Absorption Properties

In Table 2, we illustrate the effect of varying the disk model parameters. Note that for a population of infinite disks (model D1), for which we fix $R^* = 38h^{-1} \text{ kpc}$, there are no non-absorbing galaxies expected below the $R(L_K)$ line, but clearly disks must have some cut-off. As R_{cut} is reduced (models D1–D3), the fraction of non-absorbing galaxies below the $R(L_K)$ line increases, but the sensitivity in the regime $R_{\text{cut}}/R_{0.3} \sim 2$ is small. From models D4–D6, we note that the fraction of non-absorbers below the $R(L_K)$ line is not very sensitive to the choice of α . An inhomogeneous population with $1.5 \leq R_{\text{cut}}/R_{0.3} \leq 2$ and $1.0 \leq \alpha \leq 2.0$ would yield a similar fraction of non-absorbers $f_{\text{below}} \sim 0.70\text{--}0.75$, provided that all galax-

ies can be characterized by $R(L_K) = R^*(L_K/L_K^*)^{0.15}$. Again, a realistic single population model must be consistent with the observed distribution $n(W_0)dW_0$ with power $\delta \simeq 1.65$. Models D7–D9 illustrate the level at which α , σ , and R_{cut} can be adjusted while still successfully recovering the $n(W_0)dW_0$ distribution and showing how the absorption properties vary between these models. We select these models for further discussion in the following sections.

Using the same criterion as for spheres, we present the distributions of D versus L_K for three realizations selected from model D8 (58 absorbers and 58 non-absorbers) in Figs. 2(d–f). The fraction of galaxies above the $R(L_K)$ line that produce absorption is larger than $f_{\text{above}} = 0.15$ for all cases in Table 2. If R_{cut} is reduced further (below 1.5), f_{above} can be reduced, but then the expected fraction of non-absorbing galaxies below the $R(L_K)$ becomes much larger. It is difficult to design a realistic disk model that will not produce a non-negligible fraction of absorbing galaxies above the $R(L_K)$ line. Physically, this is because of lines of sight that pass through the disk at large impact parameters, but also at large inclinations.

We also present the W_0 versus D distribution for 58 absorbers from model D8 in Figs. 3(d–f). As with the spherical models, the W_0 versus D distribution is qualitatively consistent with the S95 data, except that our disk models yield a deficiency of small W_0 at small D . This is an artifact of our model design, which does account for increased pathlength through highly inclined disks using a geometric scaling, but does not account for material *physically* distributed above or below the disk plane (eg. thick disk or warp material). In a more realistic model, lines of sight at small impacts that graze highly inclined galaxies with some absorbing gas distributed at $\sim 5 - 10$ kpc about the disk plane [as is likely for the Galaxy (Diplas & Savage 1991)] would also exhibit absorption, filling in the lower left corner of the $W_0 - D$ distribution. It is interesting to note that in S95 most (if not all) of the absorbers with $D \leq 15h^{-1}$ kpc are Damped Ly α (DLA) absorbers. This may imply that most DLA absorbers are highly inclined disks, and that, in view of our model interpretations, extended material above and below the disk is further implied by their detection.

3.3. Ruminations on an Unbiased Sample

The bottom line is that, regardless of the overall geometric cross-section, it is difficult to design models of absorbing gas which (1) consist of physically distinct clouds as opposed to a smooth distribution of gas that would exhibit a tighter $W_0 - D$ relationship than is observed, (2) recover the distribution of equivalent widths $n(W_0)dW_0$, and (3) yield covering factors near unity down to the required equivalent width limit within some well defined luminosity dependent galactocentric radius.

We note that none of our spherical cloud models can yield few non-absorbing galaxies at impact parameters $D \leq R(L_K)$, qualitatively reproduce the observed $W_0 - D$ distribution, and be made consistent with the observed equivalent width distribution. The basic problem is that gaps in covering result from instances of zero clouds along the line of sight. This could be adjusted by increasing the number of clouds, but then the equivalent width distribution is skewed toward large values. Decreasing the minimum equivalent width of an individual cloud could help with this discrepancy, but this would not be consistent with the small observed number of absorbers with $W_0 < 0.3 \text{ \AA}$. For disks, we note that taking into account the increased pathlength for inclined disks does in fact reduce the number of non-absorbers at small impact parameters. Indeed, our disk absorber models yield similar fractions of non-absorbers below the $R(L_K)$ line as do our spherical absorber models. In the S95 sample, only three absorbing galaxies are observed above the $R(L_K)$ line. Although some spherical cloud models appear to be relatively consistent with this result, all of our disk models predict larger numbers of absorbers at large impact parameters.

We must address the fact that our models yield no definitive boundary between absorbing and non-absorbing galaxies in the $R(L_K) - L_K$ plane. It is important to take into account that the results we have discussed so far apply to an “unbiased sample” of QSO fields. For our unbiased sample, there does appear to be a difference between the predictions for spherical and disk models. It is *in principle* possible to design a spherical cloud model that predicts very few absorbing galaxies above the $R(L_K)$ line. Whether such a model is practically realistic, effectively whether there is a sharp cut-off in radius for the existence of absorbing clouds, depends upon the details of ionization physics and on the variations in the

confining pressure and cloud properties with radius. However, none of our disk models produce a negligible fraction of absorbing galaxies above the $R(L_K)$ line, and we argue that all disk models would produce some absorbing galaxies at large impact parameters.

In a unbiased sample of QSO fields (chosen without regard to the presence or non-presence of absorption) in which all galaxy redshifts and luminosities are measured to some limiting rest L_K , our “clumpy” models predict that there is no definitive boundary between absorbing and non-absorbing galaxies. We will show in §4, that a careful “application” of the SDP selection procedures to our model fields brings our results, for both spherical and disk models, into plausible agreement with observations.

4. Confronting Observations

The SDP sample is not an unbiased sample of QSO fields, but includes 51 “absorber fields” that exhibit MgII in the redshift range $0.3 \leq z \leq 0.9$ and 25 “control fields”, in which absorption is not detected. In order to better understand the effects of biasing in the sample, we studied Monte-Carlo *fields* of spherical models S2, S11, and S12 and of disk models D7, D8, and D9. An important (and not all that certain) parameter is the mean number of galaxies per field (within the redshift range). N_{field} can be estimated from the number of *absorbers* observed per unit redshift, roughly $dN/dz = 0.85 \pm 0.2$ (Steidel & Sargent 1992) in the range $0.3 < z < 0.9$, which translates to $N_{\text{los}} = 0.51 \pm 0.12$ absorbing galaxies per line of sight. From Tables 1 and 2, we find that our simulations predict that the fraction of absorbing galaxies per line of sight is $0.46 \leq f_{\text{abs}} < 0.54$. Thus, the predicted average number of galaxies per field is $N_{\text{field}} = 0.51/f_{\text{abs}} = 0.95 - 1.10$. We adopt $N_{\text{field}} = 0.95$, but note that the observational constraint on N_{los} allows some flexibility in this quantity.

We generated 10000 simulated SDP surveys, each having 51 absorber fields and 25 control fields. The galaxies themselves were randomly selected from the models discussed in §3 (including redshifts). Based upon the presence or non-presence of absorption above the 0.3 \AA survey limit, we designated a field as an “absorber” or “control” field. Predictions based upon both the spherical and disk models are quite similar, and we thus discuss the simulation results more generally. For $N_{\text{field}} = 0.95$ we find that 38–41% of the fields ($F_{\text{abs}} = 0.36 - 0.40$) contain at

least one absorbing galaxy. This is a much smaller fraction of absorbing fields than selected in the SDP sample ($51/76 = 0.67$), which may be telling us something about our models or about a selection bias in the SDP survey. Simulated absorber fields contain on average 1.24–1.28 absorbers and 0.44–0.51 non-absorbers [control fields contain the same number of non-absorbers (0.44–0.51), as they should since the presence of an absorber does not affect the probability of finding other galaxies in the field at different redshifts]. On average, the six geometric models yield 63–65 absorbers and 33–39 non-absorbers. The observed number of non-absorbers (14) is not consistent (smaller) with the predictions of our models, and the number of absorbers observed (58) is somewhat improbable, on the low end of the tail of the distribution. In Fig. 4(a), we illustrate the simulated distributions of the number of absorbers and non-absorbers for model D8 in an “SDP survey”, in which all galaxies within a $10''$ field have been included. In this figure, we also present the number of non-absorbers with impact parameters less than $8''$ which lie below the $R(L_K)$ line. For this sub-sample, the predicted number non-absorbers approaches the observed number, providing a powerful illustration of how sensitive observational results are to observational completeness and selection effects.

4.1. Effects of Covering Factor and Selection Bias

It turns out that the numbers of absorbers, non-absorbers, and the fraction of absorbing fields F_{abs} are sensitive to the parameter N_{field} . In Table 3, we illustrate the effect of decreasing N_{field} for models D8 and S12 (other models produce similar numbers). As illustrated in Fig. 4(b) for model D8 and $N_{\text{field}} = 0.65$, the 51 model fields yield a mean of $N_{\text{abs}} = 59 - 61$ absorbers, consistent with the 58 observed by SDP.

A value of $N_{\text{field}} = 0.65$ is not implausible. If the observed dN/dz is about $1-\sigma$ smaller, we recover $N_{\text{field}} = 0.65$. Alternatively, the estimate of N_{field} scales inversely with the fraction of galaxies in the fields that produce absorption, f_{abs} . If we had designed models that yield nearly unit covering factor, we would have increased f_{abs} and provided a means to reduce N_{field} . However, this would yield an increased number of absorbing galaxies observed in 51 absorbing fields. *Galaxy models that yield higher covering factors cannot be made consistent with the number of absorbing galaxies observed by SDP.* Provided our

models statistically represent the absorption properties of real galaxies, F_{abs} of an unbiased sample of fields may be as small as 0.28, and the SDP sample may have selected heavily in favor of absorbing fields.

However, even with $N_{\text{field}} \sim 0.65$, our models predict that the observed number of 14 non-absorbing galaxies is somewhat improbable. Since the observational procedures of SDP would often miss galaxies at large angular separations, it is more instructive to focus on the fact that SDP find only two non-absorbing galaxies below the $R(L_K)$ line separating absorbers and non-absorbers. We will show that this observational result can be statistically reconciled with our simulations for both spherical and disk models once we account for (1) biasing in the choice of fields and in the practical procedure employed by SDP to obtain follow-up redshifts of galaxies, and (2) the uncertainty that even a small fraction of the absorbing galaxies may have been mis-identified (see §1).

4.2. Reconciling Selection Effects

We turn our attention to the fact that a fair number of the non-absorbing galaxies in the SDP sample do not have measured redshifts, and are therefore not represented in Fig. 2 of S95. In practice, the follow-up redshift measurements of galaxies identified in the SDP fields were implemented using the following practical considerations (Steidel, private communication). In control fields, redshifts were obtained for all galaxies within the $10''$ fields. However, in absorber fields, non-absorbers with large impacts are preferentially missing from the sample, since the search was sometimes stopped at $\sim 8''$ once a galaxy with the redshift seen in absorption had been found. In nearly all cases, redshifts were obtained for all galaxies within $8''$.

In the context of these procedures, we ask the relevant question – “for our models, what is the probability of detecting only a few non-absorbing galaxies below a statistically determined $R(L_K)$ line in a D versus L_K diagram?”. In order to address the partial coverage in the $8'' \leq D \leq 10''$ zone, we bracket the SDP procedure with two “observational scenarios”: (1) all non-absorbers with $10''$ of the QSO are included, and (2) only those non-absorbers within $8''$ of the QSO are included. In Table 4, we present the predicted mean number of non-absorbers below the $R(L_K)$ line based upon these two scenarios for the various models and for the N_{field} values 0.95 and 0.65. From the $N_{10''}$ and $N_{8''}$ entries, note that there is

not much sensitivity to the chosen observational scenario. Nonetheless, in order to best emulate the observational procedures, we applied scenario (1) to the 25 control fields and scenario (2) to the 51 absorber fields. We then computed $P(\leq 2)$, the probabilities of observing two or fewer absorbers below the $R(L_K)$ line. We find that both sphere and disk models give non-negligible probabilities for observing two or fewer non-absorbers in the SDP sample. There is a 31% chance (for spherical model S12) that SDP would detect two or fewer non-absorbers below the $R(L_K)$ line and a 5% chance for disk model D8.

Since the SDP observational procedure was to search outwards in the absorber field until a galaxy was located at the redshift seen in absorption, it is possible that some “absorbing” galaxies have actually been mis-identified [though, for several reasons, it is believed that few mis-identifications have been made (S95)]. It is likely that for each mis-identified galaxy, a non-absorbing galaxy below the $R(L_K)$ line and an absorbing galaxy above the $R(L_K)$ line would not be represented in the survey. Thus, in addition to $P(\leq 2)$, we have tabulated $P(\leq 4)$ to examine the effects of possible mis-identifications. The probability of observing four or fewer non-absorbers is not negligible for models S12 (71%), S2 (40%), and D8 (26%), for $N_{\text{field}} = 0.65$ (corresponding to $dN/dz = 0.54$). This is further illustrated by the distribution function for model D8 presented in Fig. 4. The probability of detecting four or fewer non-absorbers is not negligible in all three disk models, ranging from 16–26%.

We briefly consider the number of absorbing galaxies above the $R(L_K)$ line. In Table 5, we present the predicted numbers of absorbing galaxies above the $R(L_K)$ line and the probabilities of observing fewer than four such galaxies in an SDP sample. Both observational scenarios, eg. including all galaxies out to the field limit of $10''$ or including only those within $8''$, are presented. In particular, model S12, which is characterized by a large $N_c(0)$ and a small W_{min} , results in a large $P(\leq 4)$. As such, it yields the properties of a “sharp boundary”. For disk models, there are an abundance of absorbers above the $R(L_K)$ line in a sample of $10''$ fields. For $N_{\text{field}} = 0.65$, model D8 predicts a mean of 11 absorbing galaxies above the line, but only 5 of these are within $8''$ of the center of the field and thus certain to be included in the observational sample. If the observational procedures have lead to a bias against detecting absorbing galaxies at 8 – $10''$ then all models have a non-negligible $P(\leq 4)$.

4.3. Discussion

Based upon our models and a study of the covering factor issues implied by the Holmberg-like relationship for absorbing gas cross-section, we cannot distinguish whether MgII absorption arises primarily within clouds distributed in a spherical halo or distributed in a flattened thick disk. Both of these geometric models appear plausible with the existing data once we include uncertainties due to possible mis-identifications and a possible bias in field selection of too few non-absorber fields. The number of non-absorbing galaxies observed at small impact parameters depends strongly on how far a sample of QSO fields is from an unbiased sample. We conclude that the small observed number of non-absorbers in the SDP sample does not *necessarily* imply unity covering factor. Once observational biases and uncertainties are taken into account, the covering factor can be made consistent with 70–80%. Indeed, if the covering factor does approach unity, it is difficult to reconcile the *small* number of *absorbing* galaxies SDP observed in their 51 fields with models that match all other observational constraints.

It is clear to us that our models are idealizations of the universe of real galaxies. Our disk models do not take into account the fact that some number of halo clouds are surely present around a realistic disk galaxy. As a result, disk models yield some non-absorbers for cases where the line of sight passes too far out in an inclined disk to produce absorption (beyond R_{cut}), but some of these lines of sight might yield absorption in a galaxy with clouds in an extended halo. Likewise, our spherical “halo” models do not contribute a disk component, which would increase the number of absorbers. The implication, if we are to obtain 58 absorbers in 51 fields, is that the covering factor of the *halo proper* in such model galaxies would be reduced below $\sim 70\%$. Additionally, our models neglect the presence of satellite galaxies. Satellite galaxies, merging or otherwise, may contribute a significant cross-section for absorption (cf. York *et al.* 1986, Wang 1993). From dynamical considerations, it may be expected that absorption properties may also correlate with the presence of satellites, their distance from the primary, and the direction of their rotation with respect to the primary (prograde/retrograde). Local spiral disk galaxies are known to have an average of one to two satellites (Zaritsky *et al.* 1993). Interestingly, for their sample, the disk luminosity does not correlate with

the number of satellites, so that absorption due to satellites would not be expected to correlate with the luminosity of the primary. However, they do see the “Holmberg-effect”, in which the projected satellites show some evidence for having an excess near the minor axis of the primary. Roughly, in the case of the Milky Way, the LMC has $M_B = -18$ (and $N_H = 10^{19} \text{cm}^{-2}$ at $R = 7$ kpc) so it could have a radius for MgII absorption of ~ 25 kpc (Bowen, Blades, & Pettini 1995b), thus covering as much as $\sim 25\%$ of the halo (not including the stream!). The effect of accounting for satellite absorbers in our models would yield an increase in predicted numbers of absorbing galaxies at all impact parameters. Again, the implication, if we are to obtain 58 absorbers in 51 fields, is that the covering factor of the *halo proper* around galaxies would be reduced well below $\sim 70\%$. This would represent a significant shift in the design of our models.

It is highly unlikely that a single pre-dominant geometric cross-section can be invoked to predict the presence or non-presence of absorption. For one, it is not clear to what degree merging history plays a role in geometrically distributing *absorbing* gas. Similar merging scenarios at different redshifts might be expected to produce different absorption properties, given redshift evolution of the meta-galactic UV background and the influence of ionization on the strength of absorption and the dissipative properties of the gas. Also, it is not yet clear at what level disk/halo interactions, such as galactic fountains (Bregman 1980) or chimneys (MacLow & McCray 1988), contribute to the gas content of extended halos. Since the gas dissipation rate is density dependent, it is possible that the statistically observed cross-section of absorbers is a function of MgII column density. Gas that dissipates on a few Gyr timescale would likely infall (arising from merging, extra-galactic accretion, or disk/halo processes) onto the disk, contributing to its thickness and affecting its chemical evolution. Gas that fails to dissipate, yet maintains $\tau_{LL} \sim 1$ at a minimum, would likely remain distributed in the halo, its absorption strength being governed by the galactocentric pressure. This component of the material may not always remain bound to the galaxy. This picture has the prediction that, as seen in high resolution spectra, low column clouds should exhibit the full range of velocities across the absorption profile, often detectable in the wings of stronger lines, or suppressing the continuum between

strong lines, whereas high column clouds should have an internal velocity dispersion consistent with a population of randomly oriented disks. The consequences for inferring the presence or non–presence of absorption from a known galaxy with a given impact parameter are not clear. It may be that the statistical geometric cross–section is sensitive to the equivalent width threshold *and* the epoch from which the sample of galaxies is drawn. An W_0 threshold of 0.3 \AA at $0.3 \leq z \leq 1.0$ may sample a relative contribution from both halos and disks.

5. Testing Absorber Cross–Section and Kinematics

There are simple predictable kinematic and absorption properties that may be useful for discerning between these two geometries. Both tests require high spatial resolution imaging of the galaxies identified as absorbers. The kinematic tests also require high resolution spectra of the absorption. Both sets of data will soon be available [(HST images) Steidel & Dickinson, private communication; (HIRES/Keck spectra) Churchill (1996)].

5.1. Disk Geometry and Associated Kinematics

Absorption associated with galaxy disks is likely to exhibit the characteristic signature of rotating galaxies (cf. Lanzetta & Bowen 1992). As such, correlations between the strength and variation (spread) in the observed absorption with increased galaxy inclination provides a statistical test to discern absorber geometry. In Fig. 5(a), we show a scatter plot of the distribution of absorber equivalent widths W_0 as a function of galaxy inclination i . Note that nearly edge–on galaxies are predicted to have a median $W_0 \sim 2\text{--}4 \text{ \AA}$. If absorption arises primarily in the disk, the absorption exhibits a larger mean W_0 and larger spread as the galaxy becomes more inclined. If absorption is primarily generated in the spherical halos of galaxies, there is no such correlation predicted from our models.

From HST images, it will also be possible to measure the angle of the line of sight relative to the position angle of the projected galactic major axis (the equivalent of our θ). In Fig. 5(b) we illustrate that, statistically, if absorption arises in a disk geometry there should be twice as many absorbers along the major axis as along the minor axis. Non–absorbers

exhibit the opposite behavior. In a simplistic spherical case, there is no relationship between the clouds and the disk, and thus the relative number of absorbers to non–absorbers exhibits no dependence on the position angle, θ .

Establishing statistical kinematic trends will rely on accurate measurements of the absorption line sub-components and of the absorbing galaxy’s systemic redshifts. For our disk models, we have computed the difference between the line of sight velocity seen in absorption and the galaxy systemic velocity. For complex absorption profiles with several sub-components, one can think of the velocity seen in absorption as an optical depth weighted mean (Hobbs 1973). We assume this weighted mean of the absorption velocity can, on average, be represented by the line of sight component of the Tully–Fisher velocity given by $L_K/L_K^* = [V(L_K)/V(L_K^*)]^{3.2}$ (Pierce & Tully 1988, Forbes *et al.* 1995). The difference between the absorption velocity and the systemic velocity of an L_K galaxy is then

$$\Delta V/V(L_K) = (D/R) \cos \theta \sin i. \quad (7)$$

We illustrate in Fig. 6(a) that large $\Delta V/V(L_K)$ can result when the galaxy has a relatively large inclination. The distribution spread results from the various θ of the line of sight (eg. the small values at large i result when the line of sight passes close to the minor axis). Indeed, as we show in Fig. 6(b), there is a strong statistical relationship between $\Delta V/V(L_K)$ and θ . In this case, the spread is a result of various galaxy inclinations. For establishing these trends observationally, it is important to keep in mind that the accuracy of galaxy systemic redshifts can usually be measured with accuracy no greater than $\sim 30 \text{ km s}^{-1}$, but even with this uncertainty, the general trends are easily discernible for the expected $\sim 200 \text{ km s}^{-1}$ rotation speeds of galaxies.

5.2. Spherical Geometry and Infall Kinematics

A very attractive picture, in which absorbing gas is distributed in more or less a spherical geometry, is radial infall of intergalactic material. Steidel & Sargent (1992) observed that redshift evolution of the co–moving cross–section of MgII absorbers depends strongly upon the equivalent width limit of the sample. The observed distribution of equivalent widths of MgII absorbers changes such that the absorption strength becomes weaker with time. The argument

for infall (Steidel 1993b) is based upon the conclusion that this evolution is not provided by changes in ionization conditions or metallicities, since MgII absorption almost always exhibits saturation. Since the sizes of the overall absorbing regions apparently do not evolve [for $W_0(\lambda 2796) \geq 0.3 \text{ \AA}$, the cross-section is consistent with no evolution], the inference is that either the numbers or the velocities of the clouds are decreasing with time. In a spherical halo model, these ideas are further supported by the expected short lifetimes of $T \sim 10^4 \text{ K}$ clouds moving in a virialized halo (Mo 1995), so that a reservoir for replenishment of gaseous material is required to account for the non-evolving halo size over a Hubble time.

If absorption does arise from clouds distributed in a spherical halo with infall kinematics, the velocity width of the overall absorption profile should exhibit a trend with impact parameter. For smooth mass distribution the trend is quite simple, as we illustrate with the solid line in Fig. 7 for an L_K^* galaxy with $R_h = R^*$. The total velocity width is produced by the absorbing gas moving with the extreme line of sight velocities toward and away from the observer. This width is a maximum at $D = 0$ and decreases to no absorption for $D \geq R_h$. In the case of individual infalling clouds, the profile velocity width is due to the maximum velocity difference between the two most kinematically extreme clouds. For the case of a constant infall velocity (no dependence upon R), we compute the profile velocity width [normalized by $V(L_K)$] for model S2, based upon our Monte-Carlo simulations. We illustrate the results as a scatter diagram in Fig. 7. In cases of lines of sight that pass through only one absorbing cloud no point is plotted. Note that the general trend given by the smooth distribution is present, though the scatter is quite severe.

The features that are most relevant to future observations are the deficit of small profile widths at small impact parameter and of large profile widths at large impact parameter. For the case of spherical infall, we re-emphasize that such observed trends would be corroborated if there was no evidence for a dependence on the galaxy orientation. However, it is not unlikely that infall would be influenced by the non-symmetric potential of the galaxy close in (small D), even if it were dominated by dark halos at large D . If so, then the spherical case presented in Fig. 7 would still apply for large impact parameters, but the small impact parameter trends may exhibit additional scatter and show some connection to the galaxy orientation.

6. Conclusions

In this paper, we have been motivated by the central question: what is the predominant geometrical cross-section of galactic gas which is known to give rise to MgII absorption in the spectra of QSOs? It has been our aim to ascertain if a single geometric cross-section can be inferred as the general shape that governs the presence or non-presence of absorption in a given galaxy of known properties intervening to a QSO. To address this question, we have performed Monte-Carlo simulations of MgII absorption produced in either a spherical or in a disk geometry. The models were designed to recover the observed statistical properties of MgII absorbers, namely the distribution of $W_0(\lambda 2796)$, given by $n(W_0)dW_0 = W_0^{-1.65}dW_0$ (Steidel & Sargent 1992), the scatter in the $W_0 - D$ plane, and a near-unity covering factor. We assume throughout that each model represents a single population of absorbers, and used the $D - L_K$ plane and the Holmberg-like relation (Eq. 1) to compare our models to currently available observations. We find that:

1. A population of randomly oriented disks can produce a geometric cross-section comparable to that of spherical halos. The relative contribution is a function of both the disk thickness and its extent beyond the halo proper (see Fig. 1). Additionally, lines of sight that impact highly inclined disks at large radii likely yield absorption with $W_0 \geq 0.3 \text{ \AA}$, due to the increased column density along the line of sight, the increased velocity dispersion of the clouds in the disk, and material that extends even as little as 5 kpc above and below the disk (such as with warps).
2. Both spherical and disk models for which the parameters are tuned to recover $n(W_0)dW_0$, yield similar fractions of non-absorbers at impact parameters smaller than the ‘‘boundary’’ given by $R(L_K) = R^*(L_K/L_K^*)^{0.15}$. Spherical models can be designed to yield small fractions of absorbers above the $R(L_K)$ boundary, but disk models predict larger numbers due to lines of sight at large impact parameters through highly inclined disks. As a caveat, we note that the largest observed W_0 may be sampling galaxy pairs (Churchill 1996), which implies that the distribution derived from single galaxies would

have a steeper slope. The observed trend for MgII absorbers to become less strong with time (Steidel & Sargent 1992) may have some interesting implications for the questions we have attempted to address in this paper. One possible view is that a “pre-dominant geometry” in which MgII absorption arises could be changing with time (evolving population), based upon the notion that numerous and kinematically diverse optically thick clouds could be associated with halos or merging events at redshifts of $z \geq 1$ and could then be evolving into thick and warped disks at redshift $z \leq 1$ with remnants in the form of high velocity clouds still accreting at the present epoch. Such accretion is known to be occurring in the Galaxy [cf. the recently discovered dwarf galaxy in Sagittarius, Ibata, Irwin, & Gilmore (1994)], whose halo appears to *not* be dynamically mixed (Majewski 1996). Indeed, such mergers are predicted to leave detectable “streaming tails” or “moving groups” in the halo for timescales of a Gyr or more (Johnston, Spergel, & Hernquist 1995).

3. Our models qualitatively reproduce the observed $W_0 - D$ distribution (Fig. 3 in S95), which suggests that our scheme to model the “clumpy structure” of MgII absorbing gas in galaxies is appropriate, and provides some support that the covering factors predicted by our models are likely to be fairly accurate. We find that the small number of observed non-absorbers in the SDP sample does not *necessarily* imply near-unity covering factor to the equivalent width limit $W_0(\lambda 2796) = 0.3 \text{ \AA}$, but can be consistent with covering factors as small as 70–80%. In the case of disks we can think of an *effective* covering factor determined by considering a population of randomly oriented disks. If MgII absorbing galaxies do indeed have covering factors approaching those predicted by our models, then the 58 absorbers detected by SDP in 51 QSO fields imply that the number of galaxies per $10''$ QSO field may be as small as ~ 0.65 in the redshift regime $0.3 \leq z \leq 0.9$ in which case dN/dz is $\sim 1-\sigma$ smaller than the observed value. Spherical cloud models with larger covering factors cannot be made consistent with the observed $n(W_0)dW_0$ and $W_0 - D$ distributions and also reproduce as *few* as 58 absorbers in 51 fields in our “SDP survey” simulations.
4. Since our models are either entirely “halo” or “disk”, they both likely *under predict* the number of observed absorbers. The implication is that the halo “component” of a model incorporating both disk and halo would necessarily have a covering factor $\leq 70\%$, if we are to obtain 58 absorbers in our 51 simulated absorber fields. In our simulations, we find a gap in the $W_0 - D$ plane at small W_0 for highly inclined disks at small impact parameters ($D \leq 15h^{-1}$ kpc). We attribute this to the fact that our model disks are not *physically* extended above or below their plane. Since most or all observed absorbers in this impact regime are DLAs (S95), and since we infer that these absorbing galaxies indeed have “thick” disks based upon our models, we suggest that many of the small impact DLAs arise from highly inclined thick disks.
5. Our models, which are an unbiased sample of QSO fields in which all galaxy redshifts are “measured” to a limiting L_K , generally yield no clear boundary between absorbing and non-absorbing galaxies. This is consistently true for disk models, but for spherical models the “distinctness” of the boundary depends strongly on parameter choices. A paucity of absorbers above the $R(L_K)$ line could be used to argue against a disk geometry. But we note that a relatively larger number of absorbers above the line could be consistent with either geometry.
6. Using the the observed number of non-absorbing galaxies that fall below the $R(L_K)$ line in S95 as a discriminant between a population of spherical (halo) absorbers and disk absorbers, we find that, once we account for (1) possible selection biases toward absorbing fields, and, (2) possible mis-identifications of a few galaxies, we cannot definitively distinguish which geometry governs the presence or non-presence of absorption. We find that the probability for detecting only a few non-absorbers below the $R(L_K)$ line is not negligible for either our sphere or disk models. The final results of the SDP survey, of which S95 is only a preliminary report, are likely to provide a demanding test for the validity our models. In principle, the number of absorbing galaxies that fall above the $R(L_K)$ line may be used as a discriminant as well, with small numbers inconsistent with a disk cross-section but consistent

with certain spherical cloud models. A complete unbiased sample would allow a more robust measure of the fraction of absorbing galaxies both *above* and *below* the $R(L_K)$ line.

7. Upcoming high spatial resolution images (HST) of the absorbing galaxies and high resolution spectra (few km s^{-1}) promise to provide the necessary data to settle the issue of how MgII absorbing gas is distributed in and around galaxies. In particular, if absorption does arise in the disks of galaxies, both the disk inclination and the angle subtended between the location of the line of sight on the plane of the sky and the galaxy major axis are expected to be strongly correlated with presence of absorption and with the velocity difference between the absorption centroid and the galaxy itself (see Fig. 5). If absorption arises purely within halo clouds (infalling or otherwise kinematically distinct from the disk), no such trends with disk orientation are expected. No doubt, there will be examples of each, and of both together in a single system. The real issue we have attempted to address is which one statistically governs the prediction of absorption or non-absorption, since this should yield important clues about the origin and fate of gas for theories of galaxy evolution. For clouds infalling into spherical halos, the width of the overall absorption profile is expected to decrease with increasing impact parameter (see Fig. 7), though the scatter can be quite large in the regime $20 \leq D \leq 40 h^{-1}$. Until these observations and tests are investigated, we submit that the standard picture of a spherical distribution of halo clouds around galaxies is not necessarily required by existing data. Since, at intermediate redshifts, MgII absorption may be present in the disks of galaxies out to radii at which HI drops below 10^{17} cm^{-2} , we suggest that MgII disks are quite likely to make a substantial contribution to the population of MgII absorbers.

In the real universe it is likely that both spherical and disk geometries contribute to the MgII cross-section, and that no single geometric configuration of discrete absorbing clouds can be identified as being solely responsible for MgII absorbers. If this is true, then the apparent boundary in the $D - L_K$ plane, which provides compelling evidence suggestive of a

mechanism for a K luminosity (mass) dependent cut-off in absorbing galaxies, may indeed result from small number statistics.

As an example of how varied absorption conditions may be, consider three possible lines of sight through a disk galaxy: 1) A line of sight close ($< 10\text{--}20$ kpc) to the center of a modestly inclined spiral galaxy must pass through the disk and may pass through halo clouds or satellite galaxies. If the inclination is large, then for absorption to be strong, the disk would likely have extended material above or below the plane. 2) If the line of sight passes at larger impact parameter through a modestly inclined disk galaxy, then the question of the origin of MgII absorption is more controversial. It becomes a question of whether the HI disk extends far enough beyond the optical radius of a galaxy and/or whether the halo has a significant covering factor of clouds, high velocity or otherwise. The relative importance of these two contributions may change with redshift. 3) Very large impact lines of sight will pass too far out in an inclined disk galaxy for absorption from the disk itself to dominate. In these cases, an absorption line may still result from halo clouds or from satellites or satellite debris and would likely be optically thin. Though there are contributions to absorption profiles from multiple components in galaxies and their surroundings, a general geometric cross-section for absorption may still be definable. Chances are that this will be a function of the MgII equivalent width threshold, or actually, of the column density “contour”. Progress on defining the contributions of halos and disks to these cross-sections is forthcoming through high-resolution imaging, while the specific details of what galaxy components combine to produce absorption will rely on their signatures in high-resolution spectra.

This work was supported in part by NASA grant NAGW-3571 at Penn State and by the National Science Foundation under Grant No. PHY94-07194 through the ITP. CWC would like to acknowledge partial support from the California Space Institute under a grant issued to S. Vogt. It is a pleasure to thank our colleagues D. Bowen, S. Charlot, R. Ciardullo, S. Horner, K. Lanzetta, D. Meyer, C. Norman, P. Shapiro, and J. van Gorkom, for their insights. We are grateful to Chuck Steidel and Mark Dickinson for detailed discussions regarding the selection procedures implemented during their MgII absorbing galaxy study.

REFERENCES

- Bahcall, J.L., and Spitzer, L, Jr. 1969, ApJ, 156, L63
- Bechtold, J., and Ellingson, E. 1992, ApJ, 396, 20
- Bergeron, J., and Boissé, P. 1991, A&A, 243, 344
- Bergeron, J., and Stasińska, G. 1986, A&A, 169, 1
- Bergeron, J. *et al.* 1994, ApJ, 436, 33
- Bowen, D.V., Blades, J.C., and Pettini, M. 1995a, ApJ, in press
- Bowen, D.V., Blades, J.C., and Pettini, M. 1995b, ApJ, in press
- Bregman, J. 1980, ApJ, 236, 577
- Cardelli, J.A., Sembach, K.R., and Savage, B.D. 1995, ApJ, 440, 241
- Cen, R., Miralda-Escudé, J., Ostriker, J.P., and Rauch, M. 1994, ApJ, 427, L9
- Churchill, C.W. 1996, UCSC PhD thesis, in preparation
- Churchill, C.W., Vogt, S.S., and Steidel, C.C 1995 in QSO Absorption Lines, ed. G. Meylan (Springer Verlag : Garching), 153
- Corbelli, E., and Salpeter, E.E. 1993, ApJ, 419, 104
- Corbelli, E., Schneider, S.E., and Salpeter, E.E. 1989, AJ, 97, 390
- Diplas, A., and Savage, B.D. 1991, ApJ, 377, 126
- Dove, J.B., and Shull, J.M. 1994, ApJ, 423, 196
- Drinkwater M.J., Webster, R.L., and Thomas, P.A 1995, in Quasar Absorption Lines, ed. G. Meylan, (Garching : Springer-Verlag), 165
- Ferland, G.J. 1988, Ohio State University Department Internal Report, 87-001
- Forbes, D.A., Phillips, A.C., Koo, D.C., and Illingworth, G.D. 1995, ApJ, submitted
- Hobbs, L.M. 1973, ApJ, 180, L79
- Hoffman, G.L., Lu, N.Y., Salpeter, E.E., Farhat, B., Lamphier, C., and Roos, T. 1993, AJ, 106, 39
- Holmberg, E. 1975, in Stars and Stellar Systems, 9, Galaxies and the Universe, ed. A. Sandage, M. Sandage, and J. Kristian, (Chicago: University of Chicago Press), 123
- Ibata, R.A., Irwin, M.J., and Gilmore, G. 1994, Nature, 370, 194
- Irwin, J.A. 1995, PASP, 107, 715
- Johnston, K.V, Spergel, D.N, and Hernquist, L. 1995, ApJ, 451, 598
- Lanzetta, K.M., and Bowen, D.V. 1992, ApJ, 391, 48
- Lanzetta, K.M., and Bowen, D.V. 1990, ApJ, 357, 321
- Lu, L., Savage, B.D., and Sembach, K.R. 1994, ApJ, 426, 563
- MacLow, M.M, and McCray, R. 1988, ApJ, 324, 776
- Majewski, S. 1996, in Formation of the Galactic Halo... Inside and Out, eds. A. Sarajedini and R. Zinn, (PASP Conference Series), to preparation
- Maloney, P. 1992, ApJ, 398, L89
- Maloney, P. 1993, ApJ, 414, 57
- Mo, H.J. 1995, in Quasar Absorption Lines, ed. G. Meylan, (Garching : Springer-Verlag), 445
- Petitjean, P. and Bergeron, J. 1990, A&A, 231, 309
- Pierce, M.J., and Tully, R.B. 1988, ApJ, 330, 579
- Rauch, M., and Haehnelt, M.G. 1995, MNRAS, submitted
- Salpeter, E.E. 1993, AJ, 106, 1265
- Salpeter, E.E. 1995, in The Physics of the Interstellar Medium and Intergalactic Medium, ed. A. Ferrara, C. Heiles, C. McKee, and P. Shapiro, (PASP Conference Series), in press
- Salpeter, E.E., and Hoffman, G.J. 1995, ApJ, 441, 51
- Sargent, W.L.W., Steidel, C.C, and Boksenberg, A., 1988, ApJ, 334, 22
- Sargent, W.L.W., Boksenberg, A., and Steidel, C.C 1988, ApJS, 68, 539
- Savage, B.D. *et al.* 1993, ApJ, 413, 116

- Savage, B.D., Lu, L., and Sembach, K.R. 1995, ed. G. Meylan, (Garching : Springer-Verlag), 119
- Sembach, K.R., Savage, B.D., and Lu, L. 1995, ApJ, 439, 672
- Shandarin, S.F., Melott, A.L., McDavitt, K., Pauls, J.L., and Tinker, J. 1995, Phys. Rev. Lett., 75, 7
- Steidel, C.C. 1995, in Quasar Absorption Lines, ed. G. Meylan, (Garching : Springer-Verlag), 139
- Steidel, C.C. 1993, in The Environment and Evolution of Galaxies, ed. J.M. Shull and H.A. Thronson, (Kluwer: Dordrecht), 263
- Steidel, C.C. 1993, in Galaxy Evolution: The Milky Way Perspective, ed. S. Majewski, (PASP Conference Series), 49, 227
- Steidel, C.C., Dickinson, M., and Persson, S.E. 1994, ApJ, L75
- Steidel, C.C., Dickinson, M., and Persson, S.E. 1996, in preparation
- Steidel, C.C., and Sargent, W.L.W. 1992, ApJS, 80, 1
- Wolfe, A.M., Fan, X.-M., Tytler, D., Vogt, S.S., Keane, M.J., and Lanzetta, K.M. 1994, ApJ, 435, L101
- van Gorkom J.H. *et al.* 1993, AJ, 106, 2213
- Vogt, S.S. *et al.* 1994, SPIE, 2198, 326
- Wang, B. 1993, ApJ, 415, 174
- York, D., Dopita, M., Green, R., and Bechtold, J. 1986, ApJ, 311, 610
- Yun, M.S., Ho, P.T.P., and Lo, K.Y. 1994, Nature, 372, 530
- Zaritsky, D., Smith, R., Frenk, C., and White, S.D.M. 1993, ApJ, 405, 464

TABLE 1
EFFECT OF THE VARIATION OF PARAMETERS FOR SPHERE MODELS

Model (1)	Model Parameters				Absorption Properties				
	α (2)	σ (3)	N_c (4)	W_{\min} [Å] (5)	R^* [kpc] (6)	f_{abs} (7)	f_{below} (8)	f_{above} (9)	δ (10)
S1	0.0	0.2	3	0.30	34	0.46	0.76	0.08	2.3
S2	0.5	0.2	3	0.30	35	0.48	0.78	0.09	1.8
S3	1.0	0.2	3	0.30	35	0.47	0.79	0.08	1.4
S4	2.0	0.2	3	0.30	36	0.48	0.80	0.10	1.2
S5	1.0	0.4	2	0.30	37	0.46	0.66	0.22	2.1
S6	1.0	0.4	3	0.30	35	0.47	0.78	0.09	1.4
S7	1.0	0.4	6	0.30	36	0.53	0.93	0.03	0.4
S8	0.0	0.4	6	0.15	37	0.48	0.83	0.04	3.5
S9	0.5	0.4	6	0.15	37	0.48	0.84	0.04	2.1
S10	1.0	0.4	6	0.15	37	0.49	0.85	0.04	1.4
S11	2.0	0.4	2	0.30	39	0.47	0.66	0.22	1.7
S12	0.8	0.4	6	0.15	37	0.49	0.85	0.04	1.6

NOTE.— The model designation is given in column 1. Column 2 lists the index for $W(R) \sim R^{-\alpha}$ for individual clouds. The variance σ around this mean equivalent width $W(R)$ is listed in column 3. Column 4 gives the mean number of clouds along a $D = 0$ line of sight. The minimum equivalent width W_{\min} of an individual cloud is listed in column 5. Column 6 lists the value of $R(W_0 = 0.3 \text{ \AA})$ for L_K^* galaxy. Columns 7, 8, and 9 give the fraction of all galaxies in unbiased fields that produce absorption, the fraction of galaxies below the boundary that produce absorption, and the fraction of galaxies above the boundary that produce absorption, respectively. In column 10 is the best fit slope of an assumed power law to the W_0 distribution.

TABLE 2
EFFECT OF THE VARIATION OF PARAMETERS FOR DISK MODELS

Model (1)	Model Parameters			Absorption Properties				
	α (2)	σ (3)	R_{cut} (4)	R^* [kpc] (5)	f_{abs} (6)	f_{below} (7)	f_{above} (8)	δ (9)
D1	1.0	0.0	∞	38	0.91	1.00	0.79	1.5
D2	1.0	0.0	2.0	34	0.52	0.75	0.23	1.9
D3	1.0	0.0	1.5	37	0.47	0.70	0.18	1.8
D4	0.0	0.0	2.0	27	0.50	0.69	0.26	3.0
D5	1.0	0.0	2.0	34	0.52	0.75	0.23	1.9
D6	2.0	0.0	2.0	35	0.49	0.75	0.16	1.5
D7	1.0	0.4	2.0	38	0.54	0.71	0.33	1.7
D8	1.3	0.0	2.0	34	0.50	0.74	0.20	1.8
D9	1.1	0.2	1.5	40	0.50	0.71	0.24	1.8

NOTE.— The model designation is given in column 1. Column 2 lists the index for $W(R) \sim R^{-\alpha}$ for individual clouds. The variance σ around this mean equivalent width $W(R)$ is listed in column 3. Column 4 gives the cut-off radius in units of $R(W_0 = 0.3 \text{ \AA})$. The value of $R(W_0 = 0.3 \text{ \AA})$ for an L_K^* galaxy is listed in column 5. Columns 6, 7, and 8 give the fraction of all galaxies in unbiased fields that produce absorption, the fraction of galaxies below the boundary that produce absorption, and the fraction of galaxies above the boundary that produce absorption, respectively. In column 9 is the best fit slope of an assumed power law to the W_0 distribution.

TABLE 3
EFFECT OF THE VARIATION OF DENSITY OF ABSORBING GALAXIES

N_{field}	F_{abs}	Full Sample of Fields ^a		Absorber Fields ^b		Control Fields ^c	
		N_{abs}	N_{non}	N_{abs}	N_{non}	N_{abs}	N_{non}
Model D8							
0.95	0.38	64	36	1.26	0.48	0	0.48
0.80	0.33	62	30	1.21	0.40	0	0.40
0.65	0.28	60	25	1.17	0.33	0	0.33
Model S12							
0.95	0.37	64	37	1.25	0.49	0	0.49
0.80	0.32	62	31	1.21	0.41	0	0.41
0.65	0.27	59	25	1.17	0.33	0	0.33

NOTE.— N_{field} is the input mean number of galaxies per field. The fraction of fields that have at least one absorber is given by F_{abs} . For the full sample, the absorber fields, and the control fields, the N_{abs} and N_{non} denote the mean number of absorbers and non-absorbers, respectively.

^aTotal mean numbers in a sample of 51 absorber fields and 25 control fields

^bMean numbers in individual absorber fields

^cMean numbers in individual non-absorber fields

TABLE 4
 EXPECTED NUMBERS OF NON-ABSORBERS “BELOW THE $R(L_K)$ LINE”

Model	$N_{\text{field}} = 0.95$				$N_{\text{field}} = 0.65$			
	$N_{10''}$	$N_{8''}$	$P(\leq 2)$	$P(\leq 4)$	$N_{10''}$	$N_{8''}$	$P(\leq 2)$	$P(\leq 4)$
S2	9	7	0.018	0.123	6	5	0.109	0.402
S11	13	12	0.000	0.007	9	8	0.009	0.080
S12	6	5	0.110	0.412	4	3	0.314	0.712
D7	12	10	0.002	0.022	8	7	0.030	0.170
D8	10	9	0.006	0.052	7	6	0.051	0.260
D9	12	10	0.002	0.023	8	7	0.028	0.163

NOTE.— $N_{10''}$ is the mean number of non-absorbing galaxies below the line given by Eq. (1) in the text. $N_{8''}$ is the mean number of non-absorbing galaxies below the line that are within $8''$ of the QSO line of sight. $P(\leq 2)$ is the probability of observing two or fewer non-absorbing galaxies below the line, and $P(\leq 4)$ is the probability of observing four or fewer non-absorbing galaxies below the $R(L_K)$ line. To mimic the selection procedures of the SDP sample, the probabilities are computed for the number of galaxies within $8''$ of the QSO line of sight in the 51 absorber fields plus the number within $10''$ for the 25 control fields.

TABLE 5
 EXPECTED NUMBERS OF ABSORBERS “ABOVE THE $R(L_K)$ LINE”

Model	$N_{\text{field}} = 0.95$				$N_{\text{field}} = 0.65$			
	$N_{10''}$	$P(\leq 4)$	$N_{8''}$	$P(\leq 4)$	$N_{10''}$	$P(\leq 4)$	$N_{8''}$	$P(\leq 4)$
S2	6	0.322	3	0.778	5	0.375	3	0.822
S11	13	0.001	6	0.233	13	0.003	6	0.279
S12	2	0.934	1	0.992	2	0.953	1	0.994
D7	18	0.000	7	0.157	16	0.000	7	0.199
D8	11	0.008	5	0.410	11	0.016	5	0.464
D9	14	0.001	6	0.238	13	0.002	6	0.289

NOTE.— $N_{10''}$ is the mean number of absorbing galaxies above the line given by Eq. (1) in the text. $N_{8''}$ is the mean number of absorbing galaxies above the line that are within $8''$ of the QSO line of sight. $P(\leq 4)$ is the probability of observing four or fewer absorbing galaxies above the $R(L_K)$ line.

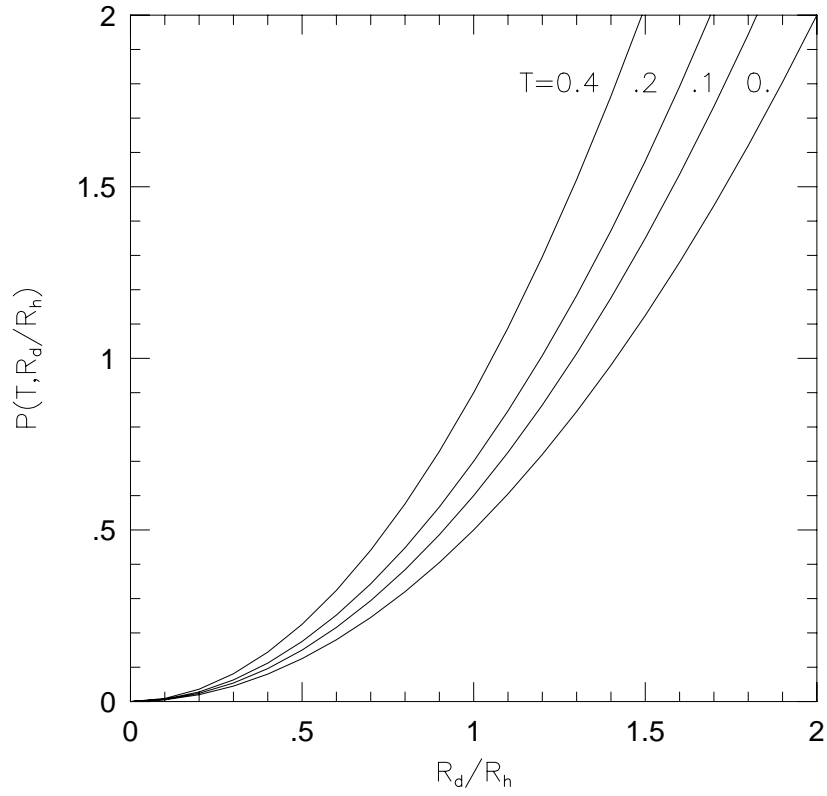


Fig. 1.— The effect of disk thickness and radius on the geometric cross-section of a population of randomly oriented disks. The vertical axis is the relative probability of intercepting a disk with thickness $T = h/R_d$ and radius R_d relative to that for intercepting a sphere of radius R_h . Here, h is the half-height of the disk. The four curves are labeled by their corresponding T .

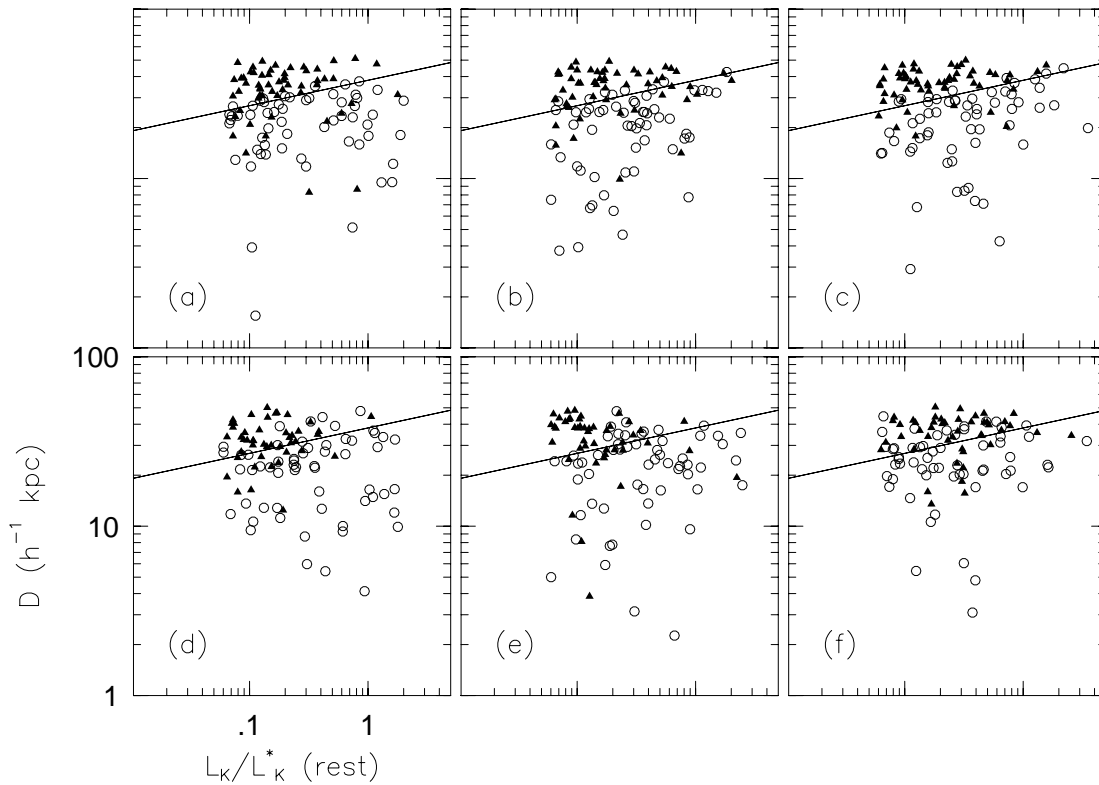


Fig. 2.— The distribution of impact parameter versus normalized K luminosity for three random realizations of the spherical model S2 (a–c) and of the disk model D8 (d–f). Open circles denote absorbing galaxies and filled triangles denote non-absorbing galaxies. These realizations sample the number of fields required to produce 58 absorbing galaxies, as observed by SDP. The model then yields the number of non-absorbers for this same number of fields, unbiased with respect to whether absorption occurs in the field or not. The solid line is the S95 best-fit to the SDP data, $D = 38h^{-1}(L_K/L_K^*)^{0.15}$ kpc, which we call the “ $R(L_K)$ line”.

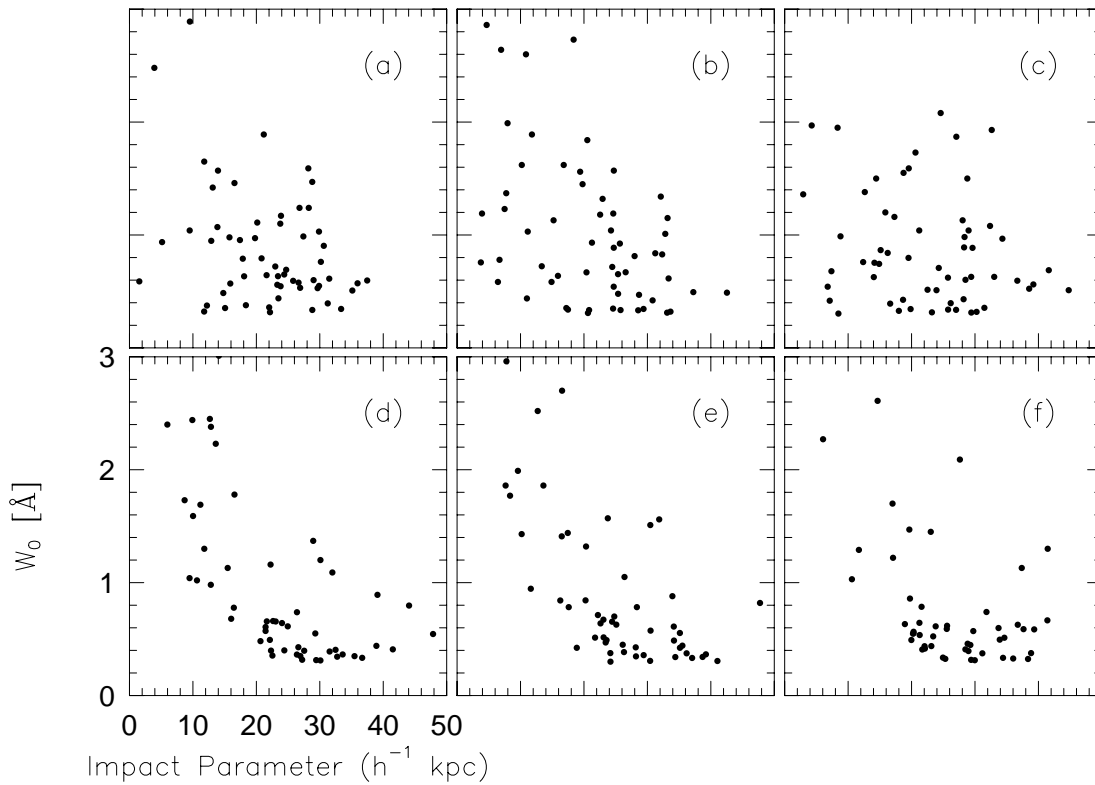


Fig. 3.— The distribution of “observed” Mg II equivalent widths W_0 versus impact D for the models presented in Figure 2. — (a–c) Three randomly selected realizations of the spherical cloud model S2. In our spheres models, the scatter in W_0 arises from clouds intercepted at different galactocentric distances and due to variations in the numbers of these clouds. — (d–f) Three randomly selected realizations of the disk model D8. For disks models, scatter is dominated by their random inclinations.

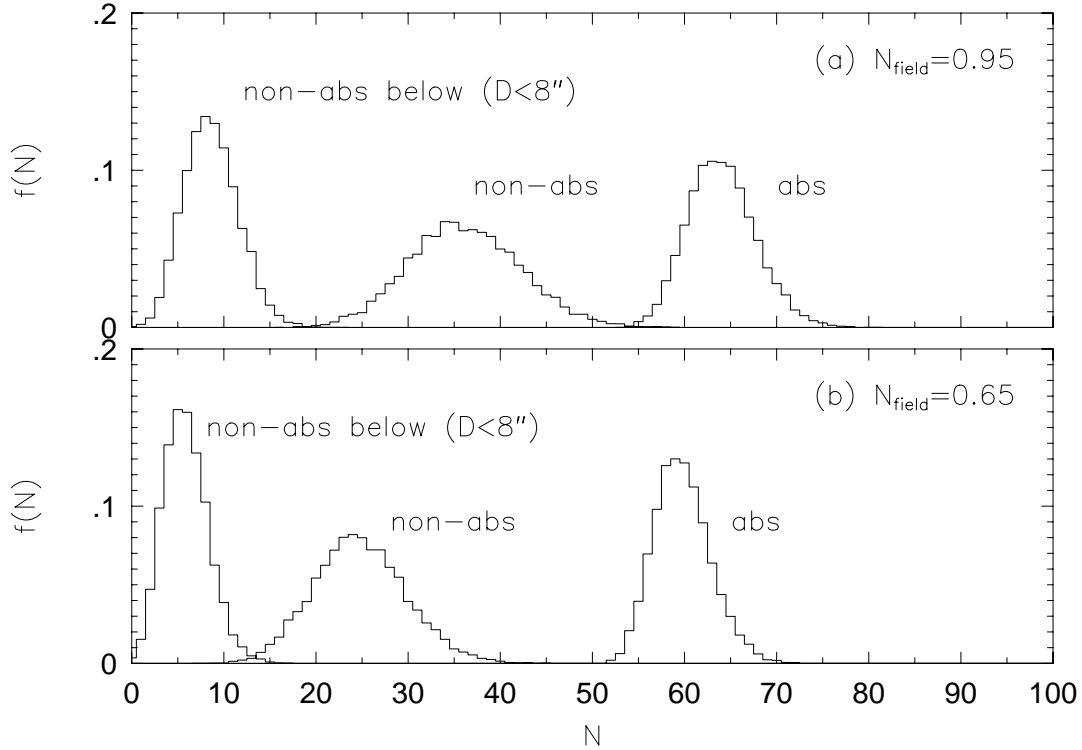


Fig. 4.— The distribution of the numbers of absorbers and non-absorbers predicted from model D8 in a sample of 51 absorber fields and 25 control fields (the simulated SDP survey). From right to left, each histogram represents (i) the number of absorbing galaxies, (ii) the number of non-absorbing galaxies, and (iii) the non-absorbing galaxies with impact parameters less than $8''$ which lie below the $R(L_K)$ line. To match observations, the mean of these distributions should be consistent with the observed numbers: 58, 14, and 2, respectively. — (a) Predicted distributions for mean of 0.95 galaxies/field. — (b) Predicted distributions for mean of 0.65 galaxies/field. The smaller number of galaxies/field provides a closer match to the observed numbers, although the numbers of non-absorbers are still on the low-end tails of the distributions predicted by our model.

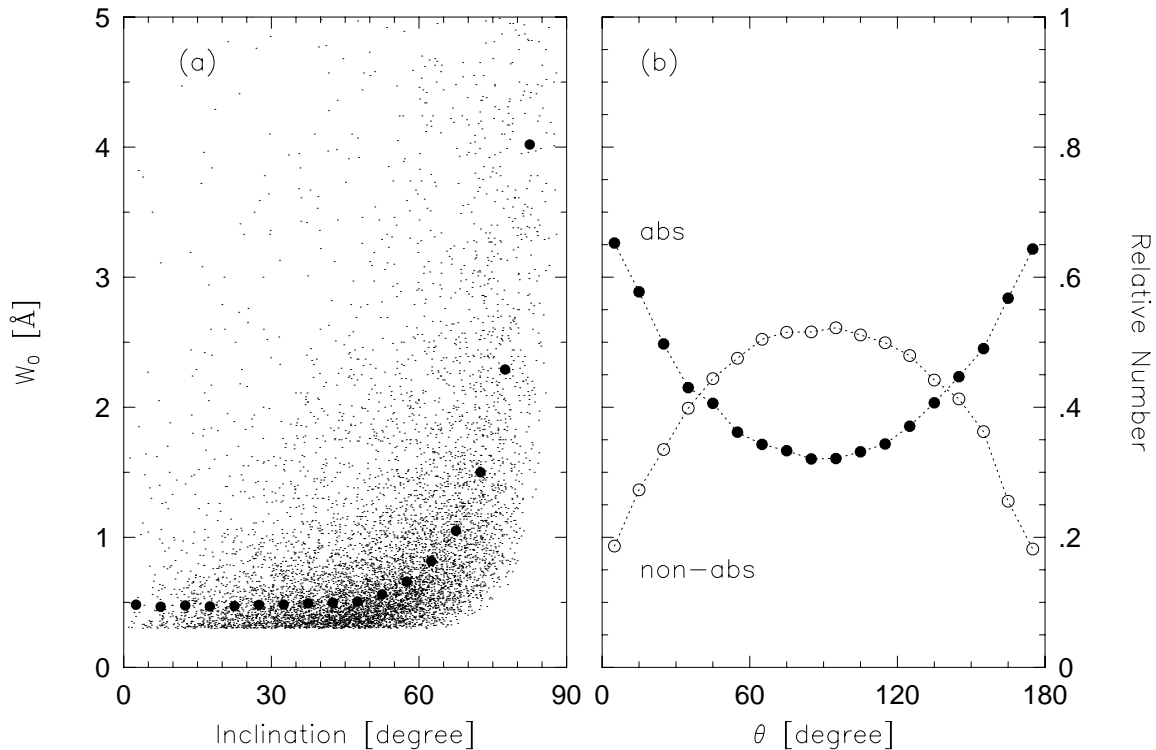


Fig. 5.— Statistical correlations between absorption strength and galaxy inclination and orientation with respect to the line of sight are predicted if the absorption is in fact associated with the galaxy disk. — (a) The trend of increasing absorption strength W_0 with disk inclination for model D8. The spread at fixed inclination is a result of a range of impact parameters. — (b) The predicted relative numbers of absorbing and non-absorbing galaxies as a function of the angle θ subtended between the sky location of the line of sight and the major axis of the oriented galaxy disk. The absorbers are denoted by solid circles and the non-absorbers by open circles. Disk models yield absorbers preferentially at angles close to the major axis, and non-absorbers to the minor axis. Spherical cloud models, such as the ones we have designed in which the velocities and numbers of clouds have no connection to the galaxy disk, produce no correlations with disk geometry.

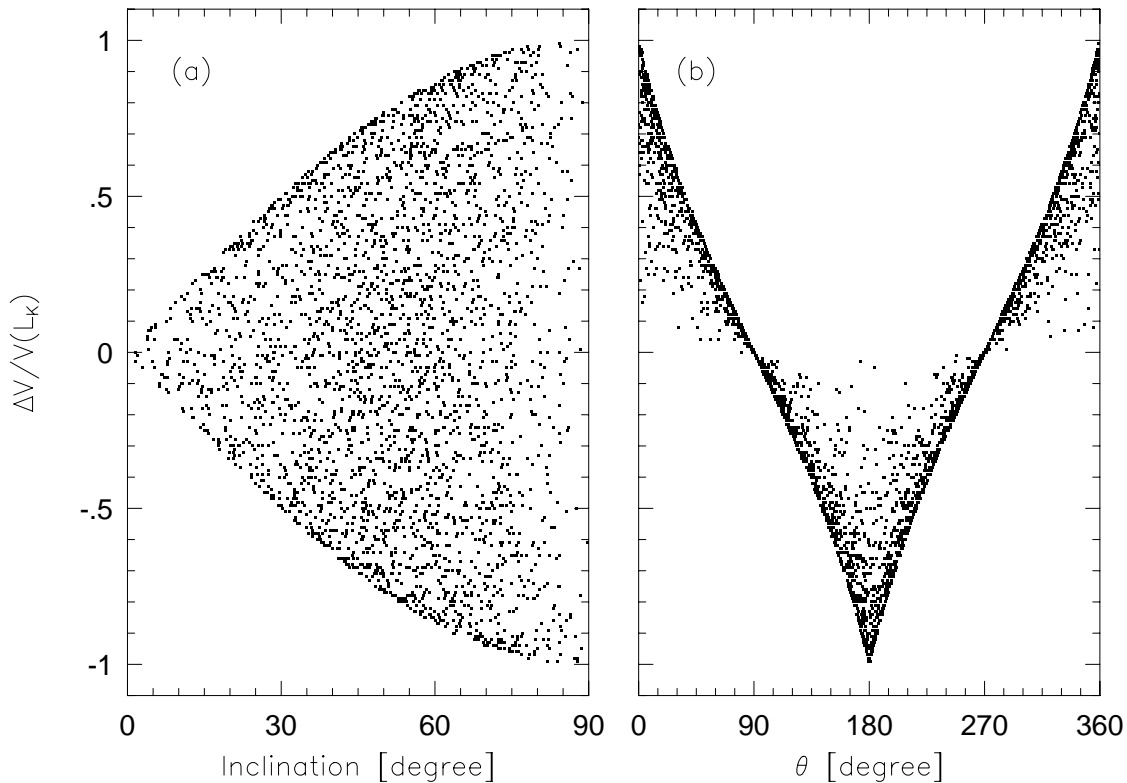


Fig. 6.— Statistical correlations between absorption kinematics and galaxy systemic velocity are predicted if the absorption arise in the extended disk. To observe such correlations will require accurate redshifts in absorption and for the host galaxy. — (a) For model D8, the weighted mean line of sight velocity of the absorption line relative to galaxy center versus disk inclination. The radial velocity is expressed in units of the rotation velocity of an L_K galaxy. The spread in observed velocity differences increases with disk inclination. — (b) The radial velocity of the absorption line relative to the center of the galaxy versus the angle θ of the LOS relative to the major axis for model D8. Scatter at a given θ results from the distribution of disk inclinations.

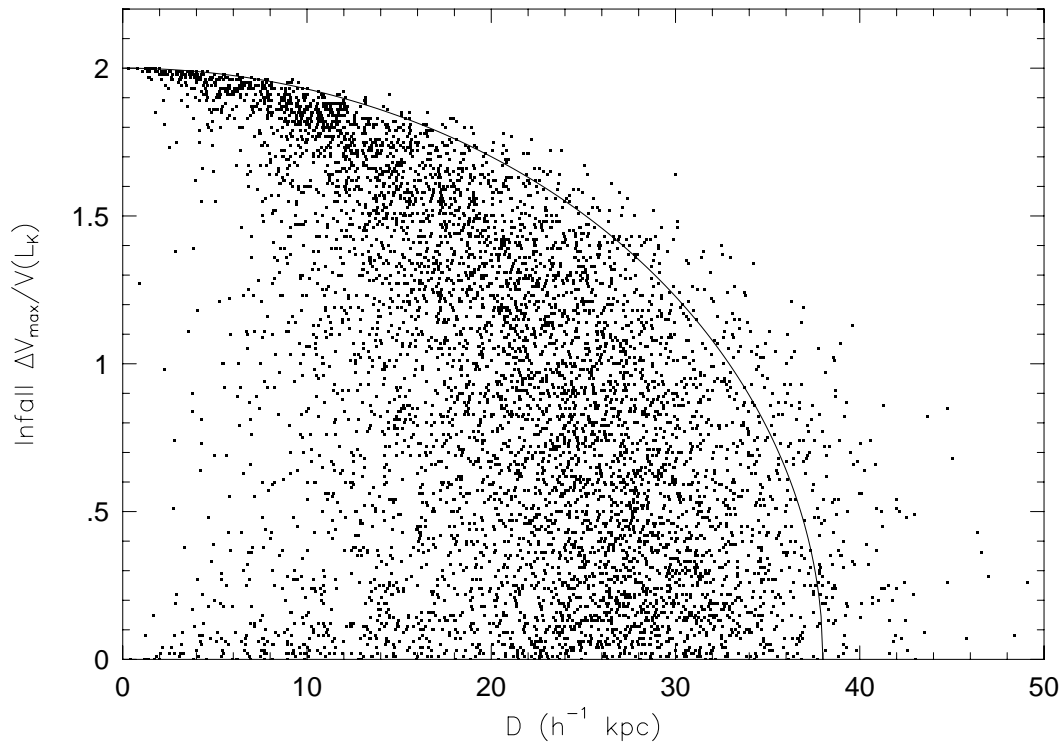


Fig. 7.— For a picture in which clouds are infalling into spherical halos with constant infall velocity, the profile velocity width (high resolution spectra) should be the maximum velocity difference between the two kinematically extreme clouds. The maximum cloud velocities intercepted along a line of sight will be correlated with impact parameter as shown here. The individual points are from Monte-Carlo simulations of model S2. At very small impact parameter the majority of the points are at nearly the maximum value of $2V(L_K)$, since the motion of the clouds is directed along the line of sight. However, occasionally due to small number statistics all clouds are moving in the same direction so that the maximum velocity difference is near zero. The solid line illustrates a smooth distribution of infalling absorbing gas for an L_K^* galaxy with $R_h = R^*$.